Available online at www.sciencedirect.com
SCIENCE DIRECT®
Applied Catalysis B: Environmental 46 (2003) 687–702
APPLIED CATALYSIS B: ENVIRONMENTAL
www.elsevier.com/locate/apcatb

On the activation of Pt/Al_2O_3 catalysts in HC-SCR by sintering: determination of redox-active sites using Multitrack

A.R. Vaccaro [a,*], G. Mul [a], J. Pérez-Ramírez [b], J.A. Moulijn [a]

[a] *Reactor & Catalysis Engineering, DelftchemTech, Delft University of Technology, Julianalaan 136, 2628 BL Delft, The Netherlands*
[b] *Norsk Hydro, Research Centre, Hydrocarbon Processes and Catalysis, P.O. Box 2560, N-3907 Porsgrunn, Norway*

Received 18 December 2002; received in revised form 27 June 2003; accepted 27 June 2003

Abstract

A highly dispersed Pt/Al_2O_3 catalyst was used for the selective catalytic reduction of NO_x using propene (HC-SCR). Contact with the reaction gas mixture led to a significant activation of the catalyst at temperatures above 523 K. According to CO chemisorption data and HRTEM analysis, Pt particles on the activated catalyst had sintered. The redox behavior of the fresh and sintered catalysts was investigated using Multitrack, a TAP-like pulse reactor. If Pt particles on the catalyst are highly dispersed (average size below ∼2 nm), only a small part (∼10%) of the total number of Pt surface sites as determined by CO chemisorption (Pt_{surf}) participates in H_2/O_2 redox cycles ($Pt_{surf,redox}$) in Multitrack conditions. For a sintered catalyst, with an average particle size of 2.7 nm, the number of Pt_{surf} and $Pt_{surf,redox}$ sites are in good agreement. Similar results were obtained for both catalysts using NO as the oxidant. The low number of $Pt_{surf,redox}$ sites on highly dispersed Pt/Al_2O_3 is explained by the presence of a kinetically more stable—probably ionic—form of Pt–O bonds on all surface sites of the smaller Pt particles, including corner, edge and terrace sites. When the average particle size shifts to ∼2.7 nm, the kinetic stability of all Pt–O bonds is collectively decreased, enabling the participation of all Pt surface sites in the redox cycles.

A linear correlation between the NO_x conversion in HC-SCR, and the amount of $Pt_{surf,redox}$ was found. This suggests that redox-active Pt sites are necessary for catalytic activity. In addition, the correlation could be significantly improved by assuming that $Pt_{surf,terrace}$ sites of the particles larger than 2.7 nm are mainly responsible for HC-SCR activity in steady state conditions. Implications of these results for the pathway of HC-SCR over Pt catalysts are discussed.

Keywords: Pt; Al_2O_3; Sintering; TAP reactor; Active site; Oxidation; Reduction; NO_x; HC-SCR; Activation

1. Introduction

Platinum-based catalysts show a high activity and stability in the selective catalytic reduction of NO_x using hydrocarbons (HC-SCR), even under adverse reaction conditions such as in the presence of water and SO_2 [1,2]. Therefore, these catalysts are attractive to use in the elimination of NO_x from car exhaust streams containing excess oxygen (lean deNO_x process) [3], especially if the high selectivity towards N_2O (70% over usual catalysts) [4] is prevented. The oxidation of the hydrocarbon, e.g. propene (Eq. (1)) is one of the two main reactions taking place in the HC-SCR process. The other is the reduction of NO (Eq. (2), with n being an integer, $9 > n > 0$).

$$2C_3H_6 + 9O_2 \rightarrow 6CO_2 + 6H_2O \quad (1)$$

* Corresponding author. Tel.: +31-15-278-1186; fax: +31-15-278-5006.
E-mail address: a.r.vaccaro@tnw.tudelft.nl (A.R. Vaccaro).

0926-3373/$ – see front matter © 2003 Elsevier B.V. All rights reserved.
doi:10.1016/S0926-3373(03)00271-6

$$2C_3H_6 + (18 + 2n)NO \rightarrow 6CO_2 + 6H_2O + (9 - n)N_2 + 2nN_2O \quad (2)$$

Under realistic lean deNO_x testing conditions (C_3H_6/NO ~1, O_2/NO ~10–100) reaction (1) is predominant [2].

Several authors have noticed an influence of the Pt dispersion on the performance of Pt-group catalysts in HC-SCR [5,6]. Burch and Millington [5] present an apparent hyperbolic relation between dispersion of the fresh catalyst and turnover frequency (TOF) in NO removal over Pt/Al_2O_3 and Pt/SiO_2 catalysts. Catalysts with a big average Pt particle size apparently exhibit a higher TOF than those with small ones. It was further shown by various research groups that highly dispersed Pt catalysts undergo sintering in HC-SCR, which is proposed to be an NO induced process [6–9].

A particle size dependency on activity of Pt catalysts has not only been observed in reactions involving the reduction of NO [10], but also in many other oxidation reactions. The rates of the oxidation of NO [11], propene [12], methane [13–15], benzene [16], and other hydrocarbons [17] are all increased as a function of increasing Pt particle size.

In general, atomic oxygen adsorbed on Pt metal surfaces is believed to be active in combustion reactions [18,19]. Three hypotheses can be put forward to explain the effect of the Pt particle size on the activity of Pt/Al_2O_3 in oxidation reactions:

1. The enhanced TOF of a Pt surface site is directly related to the decrease of the average binding energy of oxygen on the Pt particle. This view results from thermogravimetry and H_2 TPR studies [14]. Surface sites or Pt particles with different TOF are not specifically considered; the TOF of the Pt surface sites is directly enhanced by the lowered activation energy.
2. The relative abundance of specific Pt surface sites responsible for activity in oxidation reactions (e.g. terrace sites) is increased as a function of increasing Pt particle size. This is in agreement with surface science studies, which indicate that on terrace sites the stability of adsorbed oxygen is significantly less than on edge sites [20]. Various authors use this hypothesis to explain experimental results, e.g. in propene oxidation over Pt/Al_2O_3 [12].
3. The oxidation state of a platinum particle being stable under reaction conditions ranges from +IV to zero as a function of the individual particle size. That is to say that the nature of the adsorbed oxygen species changes from ionic to atomic species. This is in agreement with many authors finding Pt surface oxides with a Pt_{surf}:O stoichiometry higher than 1 on highly dispersed Pt/Al_2O_3 [21] or even complete oxidation to PtO_2 [22], whereas only larger Pt particles remain metallic under highly oxidizing conditions [23]. Various authors use this hypothesis to explain experimental results, e.g. in methane, cyclopropane and benzene oxidation over Pt/Al_2O_3 [15–17].

Please note that the two latter hypotheses do not necessarily imply a modification of the apparent activation energy. The activation rather involves an increase of the pre-exponential factor of the Arrhenius equation [16,17].

In the present contribution Multitrack was applied, an advanced TAP-like reactor system [24], to further evaluate a distinction between redox-active and inactive Pt surface sites on Pt/Al_2O_3 catalysts with different Pt dispersions. The number of redox-active sites was compared with the number of Pt surface sites determined by conventional volumetric CO chemisorption. Experiments with NO or propene were also conducted to establish the relevance of these sites for the HC-SCR reaction over Pt/Al_2O_3. Finally, the correlation between Multitrack results and the NO_x conversion in steady state HC-SCR experiments is discussed.

2. Experimental

2.1. Catalyst preparation and characterization

Extrudates of Al_2O_3 (Ketjen CK 300) were crushed and sieved, and the 106–212 μm fraction was used as the support material without further pretreatment. The catalyst was prepared by dry impregnation using an appropriate ammonia solution of $Pt(NH_3)_4(NO_3)_2$, and dried at 393 K overnight. Finally, the sample was calcined at 773 K in static air for 5 h. The catalyst contained a nominal Pt loading of 1.0 wt.%, as determined by XRF analysis.

The N_2 adsorption isotherms at 77 K were measured using a QuantaChrome Autosorb-6B analyzer. The BET method was used to determine the specific surface area of the catalyst. The pore size distribution was determined from the desorption branch of the isotherm using the BJH model [25]. Prior to the measurements, the samples were evacuated at 623 K for 16 h.

High-resolution transmission electron microscopy (HRTEM) was carried out on a Philips CM 30 T electron microscope with a LaB_6 filament as the source of electrons operated at 300 kV. Samples were mounted on a copper-supported carbon polymer grid by placing a few droplets of a suspension of ground sample in ethanol on the grid, followed by drying at ambient conditions.

Volumetric CO chemisorption was used (QuantaChrome Autosorb-1C) to determine the Pt dispersion. Prior to CO chemisorption, the samples were reduced by pure H_2 at 548 K during 2 h (30 ml min^{-1} (STP)) at ambient pressure, followed by evacuation at 548 K for 2 h and cooling down to 308 K in vacuum. Based on the amount of CO adsorbed and assuming an adsorption stoichiometry CO:Pt = 1:1, the metal dispersion and the average particle size were calculated, applying a semi-hemispherical shape of the particle.

2.2. Catalytic activity

2.2.1. Set-up

HC-SCR activity measurements were carried out in a six-flow reactor system [26], using quartz-tube fixed-bed reactors of 4 mm i.d. and 10 mm bed length at ambient pressure. A standard total flow of 62.5 ml min^{-1} (STP) and 50 mg of catalyst (particle size 106–212 μm) was used for each run (GHSV = 50,000 h^{-1}). The space time, defined as $W/F(NO)_0$, was 1.1 g s μmol^{-1}, W being the catalyst mass and $F(NO)_0$ the initial molar flow of NO. The reaction mixture consisted of 0.1 kPa NO_x, 0.1 kPa C_3H_6, 5 kPa O_2, and balance He. NO and NO_2 were continuously analyzed with a chemoluminescence analyzer (Eco-Physics CLD 700 EL), while the other gas components were discontinuously analyzed by gas chromatography. The gas chromatograph (Chrompack CP 9001) was equipped with a thermal conductivity detector and a flame ionization detector, and two columns: Poraplot Q (for separation of CO_2, N_2O, H_2O, and C_3H_6) and Molecular Sieve 5 Å (for O_2, N_2 and CO separation).

2.2.2. Procedures

Activity experiments were performed in two different ways.

2.2.2.1. Procedure A1. The catalyst was pretreated in He at 473 K for 3 h, followed by a switch to the reaction mixture described above and a stepwise increase of temperature with intervals of 20 K, up to 673 K. The increasing temperature cycle was followed by a stepwise decrease of temperature (down-cycle at 20 K intervals). Prolonged exposure of the fresh catalyst to the reaction mixture by using 10 K steps did not result in changes of the performance up to 523 K. Hence, data points up to this temperature can be assigned to the performance of the fresh catalyst (catalyst 'fresh'). Before subjecting the spent catalyst resulting from this experiment (catalyst A1) to CO chemisorption, it was calcined in static air at 573 K for 5 h in order to clean-off stable hydrocarbonaceous species formed on the catalyst surface during reaction.

2.2.2.2. Procedure A2. The catalyst was pretreated at 773 K in the reaction mixture for 3 h, followed by a stepwise decrease of temperature with intervals of 20 K. The spent catalyst (catalyst A2) was calcined in static air at 573 K for 5 h before CO chemisorption analysis.

In both procedures, at each temperature the catalyst was equilibrated for 1 h, before the products were analyzed. Under the applied experimental conditions, mass and heat transport limitations were absent. Based on the ratio between NO_x and propene conversion, defined as the hydrocarbon efficiency ($E(HC) = X(NO_x)/X(C_3H_6)$), the relative contribution of reaction (1) compared to reaction (2) (see Section 1) to propene oxidation can be determined. Turnover frequencies are calculated on the basis of the NO_x conversion and the number of platinum surface sites determined by CO chemisorption.

2.3. Multitrack experiments

2.3.1. Set-up

A detailed description of the Multitrack set-up (multiple time-resolved analysis of catalytic kinetics) is given elsewhere [24]. Various gases and gas mixtures can be dosed to the reactor by means of two high-speed pulse valves, yielding pulses of 10^{15} to 10^{17} molecules

within 100 μs. The catalytic reactor is located in a high vacuum system, and during pulsing the peak pressure remains below 3 Pa. The catalyst bed (25 or 100 mg of catalyst, pellet size 106–212 μm) is placed between two layers of SiC particles (∼250 mg SiC each before and after the catalyst bed, particle size 190–230 μm).

In the reactor, the shape and composition of the gas pulse change due to processes such as diffusion, adsorption, and reaction. At the reactor exit the reaction products are analyzed by four quadrupole mass spectrometers positioned in-line with the reactor axis. All mass spectrometers used in this study monitored one mass number with a maximum sample frequency of 1 MHz. As the signal-to-noise ratio in this system is excellent, single pulses are sufficient to obtain good peak signals. This is important, as transient phenomena due to a changing state of the catalyst may remain unobserved, when several pulse responses have to be averaged. Furthermore, the probe molecule conversion per pulse can be calculated.

The number of molecules present in each pulse was calibrated by measuring the pressure loss in a fixed volume connected to the pulse valve as a function of a large number of pulses. Depending on the type of experiment, the following masses were monitored: *m*/*e* 2 (H_2), *m*/*e* 18 (H_2O), *m*/*e* 30 (NO), *m*/*e* 32 (O_2), *m*/*e* 40 (Ar), *m*/*e* 41 (C_3H_6), and *m*/*e* 44 (CO_2).

2.3.2. Procedures

Before performing titration experiments, the catalyst was subjected to two different pretreatments.

2.3.2.1. Pretreatment M1. After inserting the fresh catalyst into the vacuum system, it was heated up to 573 K at 10 K min^{-1}. The catalyst was stabilized for 2 h. This treatment leads to catalyst M1 and was meant to preserve the structure of the fresh catalyst.

2.3.2.2. Pretreatment M2. After inserting the reactor into the vacuum system it was heated up to 773 K (10 K min^{-1}). Subsequently, the catalyst was subjected to H_2 pulses (10^{17} molecules per pulse, 1 pulse/s) for 1 h. Then, the reactor was cooled down to 573 K, and stabilized for 2 h. This treatment results in catalyst M2 and was meant to induce sintering of Pt particles in order to allow a comparison with catalyst A2.

Following these pretreatments, titration experiments were performed at temperatures between 473 and 573 K. Pure hydrogen (10^{17} molecules per pulse) was used to reduce the oxidized Pt catalyst. The catalyst is denoted as 'completely reduced' when the area under the hydrogen-signal is constant. Pulses of 20 vol.% O_2 in Ar (10^{17} molecules per pulse) were used to re-oxidize the reduced catalyst. The catalyst is denoted 'completely oxidized' when the area under the oxygen-signal is constant. Fig. 1 shows a typical result of a titration experiment. By repeating the H_2/O_2 redox cycles, it was confirmed that the oxygen uptake values were reproducible within ±10%. Changes in temperature between 473 and 573 K hardly affected the results.

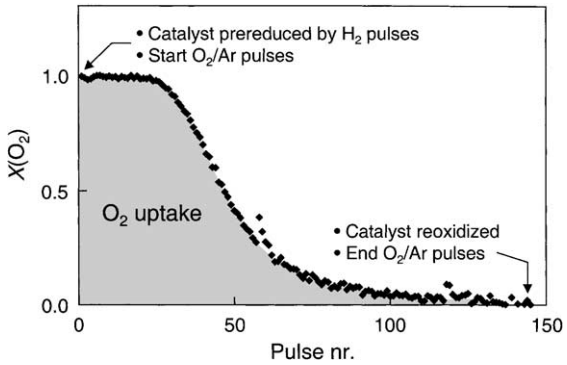

Fig. 1. Typical Multitrack titration experiment. Oxygen conversion vs. pulse number at 523 K over sample M1 after prereduction by hydrogen. Pulse composition: 20% O_2 in Ar and pulse size: $\sim 2 \times 10^{16}$ molecules.

After these reduction–oxidation experiments with H_2 and O_2, respectively, titration experiments were performed using 15 vol.% NO in Ar, and 10 vol.% C_3H_6 in Ar. After the titration experiments, the dispersion of the catalyst was determined by CO chemisorption, following the same procedures as described for catalysts A1 and A2.

Blank tests with inert material (support, SiC) showed negligible H_2 and O_2 conversion respectively uptake.

3. Results

3.1. Catalyst characterization

Characterization data of the support and the fresh catalyst are summarized in Table 1. A typical HRTEM

Table 1
Characterization data for catalysts and support used in this study

Properties	Al_2O_3	Pt/Al_2O_3	Description
Sieve fraction (μm)	106–212	106–212	After preparation
Pore volume ($cm^3\,g^{-1}$)	0.65	0.64	
S_{BET} ($m^2\,g^{-1}$)	273	269	
Mesopore size (nm)	5–10	5–10	
Pt loading (wt.%)	–	1.0	
Pt dispersion/sample fresh		0.79	After preparation
Pt dispersion/sample M1		0.73	Multitrack (without pretreatment)
Pt dispersion/sample M2		0.47	Multitrack (after H_2 pulses at 773 K)
Pt dispersion/sample A1		0.10	Activity test (feed at 453 K, *T* up/down)
Pt dispersion/sample A2		0.35	Activity test (feed at 723 K, *T* down)

Applying the BET method; derived from the application of the BJH model.

micrograph of the fresh catalyst (Fig. 2a) shows a large number of small particles of diameters between 1 and 2 nm. As the darkness of the particle decreases with size, a significant fraction of monoatomic Pt or polyatomic Pt clusters might not be visible. Very few big particles of about 10 nm size were also observed (Fig. 2b). The dispersion of the fresh catalyst as determined by CO chemisorption amounts to ∼1.3 nm, which is in good agreement with the HRTEM micrographs. The fresh catalyst consisted mainly of oxidized Pt particles, as derived from reaction of the catalyst with H_2 at room temperature. This was determined by using a TGA apparatus coupled to a mass spectrometer.

3.2. Activity evaluation

Fig. 3a and b show the conversion of NO_x and propene as determined by procedure A1 (see Section 2.2). As generally reported in the literature [2,5,6], both

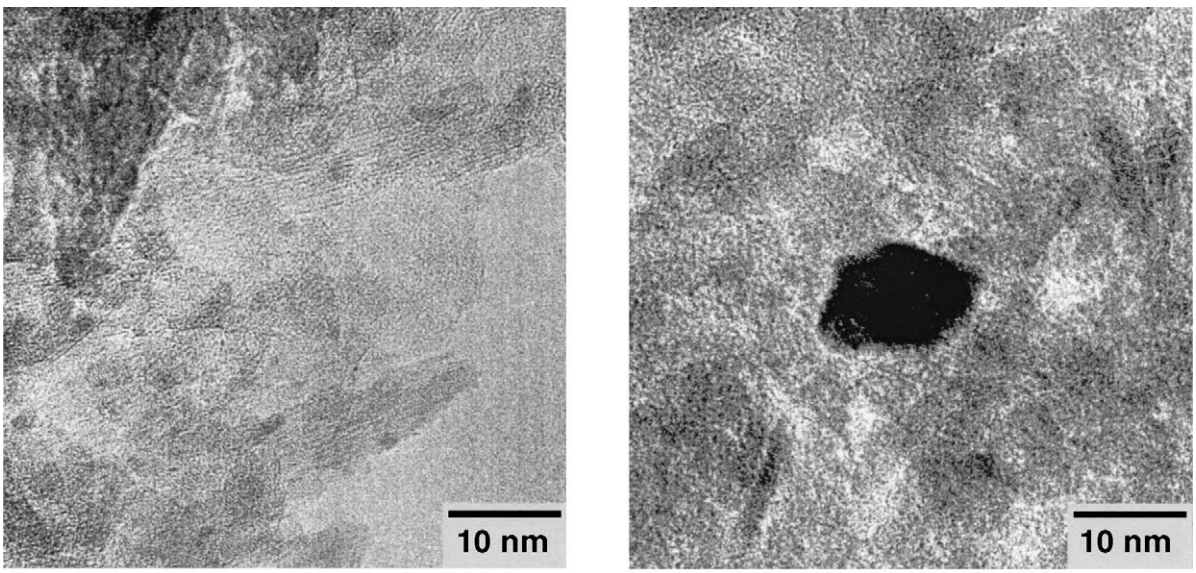

(a) (b)

Fig. 2. Representative HRTEM micrographs of the fresh Pt/Al_2O_3 catalyst: (a) typical nano-particles with size 1–2 nm and (b) one of the two metal particles found on the sample.

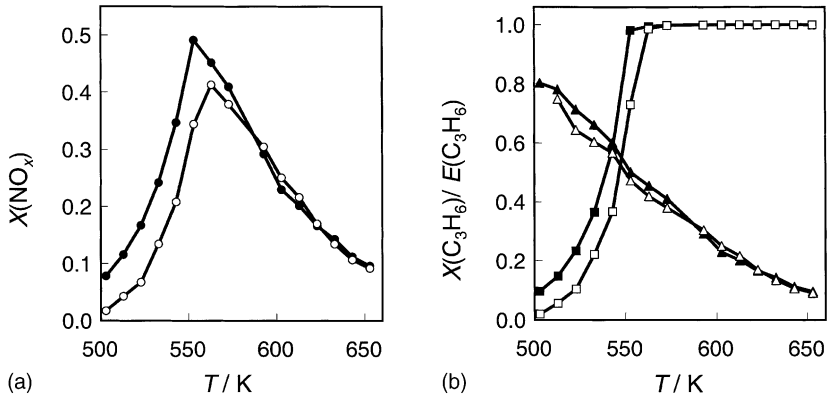

Fig. 3. Temperature dependent HC-SCR performance over Pt/Al_2O_3: (a) NO_x conversion (●, ○), (b) hydrocarbon conversion (■, □) and efficiency (▲, △). Open symbols: data during heating up-cycle of the fresh catalyst; solid symbols: data during cooling down-cycle according to procedure A1 in Section 2.2. Reaction conditions: 0.1 kPa NO_x, 0.1 kPa C_3H_6, 5.0 kPa O_2, balance He; $W/F(NO)_0 = 1.1\,g\,s\,\mu mol^{-1}$; $P = 100$ kPa.

the conversion of NO_x and propene increase steeply with temperature, until 100% propene conversion is reached at about 570 K (Fig. 3b). Above this temperature the NO_x conversion decreases (Fig. 3a). In the down-cycle, below 570 K both NO_x and propene conversion are significantly higher than in the up-cycle (fresh catalyst). The hydrocarbon efficiency E(HC) in Fig. 3b is relatively high at low temperatures and decreases almost linearly as a function of increasing temperature. Furthermore, the efficiency was not affected by the activation of the catalyst. This indicates that reaction (1) and (2) (see Section 1) are enhanced in almost an equal way. In Table 1, it is shown that due to the activity test the catalyst has sintered. The HRTEM micrograph of a spent catalyst confirms that sintering of platinum particles occurred. Many particles with sizes of 8 nm and more were identified (Fig. 4). Table 2 gives an overview of platinum dispersion data determined by CO chemisorption, and TOF data at 503 and 523 K. At this time it is not yet clear why sintering induced by experiment A2 (pretreated in the reaction mixture at 773 K) is less severe than in experiments Al (only treated at 673 K). An optimum in TOF exists for Pt particles with a dispersion of about 0.35. This will be further discussed in the following sections.

Table 2
Sintering and activation of the catalyst for HC-SCR

Catalyst	Pt_{surf} dispersion	10^{-3} TOF (s^{-1})	
		503 K	523 K
Fresh	0.79	0.4	1.2
A1	0.10	9.2	24
A2	0.35	6.2	17

Experimental conditions as described in Fig. 4. Turnover frequency (TOF) expressed as mol NO_x removed per mol of Pt in the catalyst and second (s^{-1}).

3.3. Multitrack experiments

3.3.1. Conversion of H_2 and C_3H_6 over preoxidized Pt/Al_2O_3

The hydrogen conversion curves of the catalysts M1 and M2 as a function of the H_2 pulse number at 573 K are shown in Fig. 5a. The total hydrogen consumption is much larger for catalyst M2 than catalyst M1. Treatment M2 (see Section 2.3) apparently enhances the number of oxidized Pt sites that can be reduced by hydrogen. In this paper, these sites are called $Pt_{surf,redox}$ sites. Please note, that this term is strictly related to the specific experimental conditions used in the Multitrack. It does not imply, that a more severe reduction condition (e.g. higher H_2 partial pressure, temperature, and longer exposure time like in volumetric H_2/O_2 titration) could not lead to the reduction of more Pt surface sites.

After re-oxidation of the catalysts with oxygen pulses (see later), reduction with propene was performed. Fig. 5b shows that also the number of

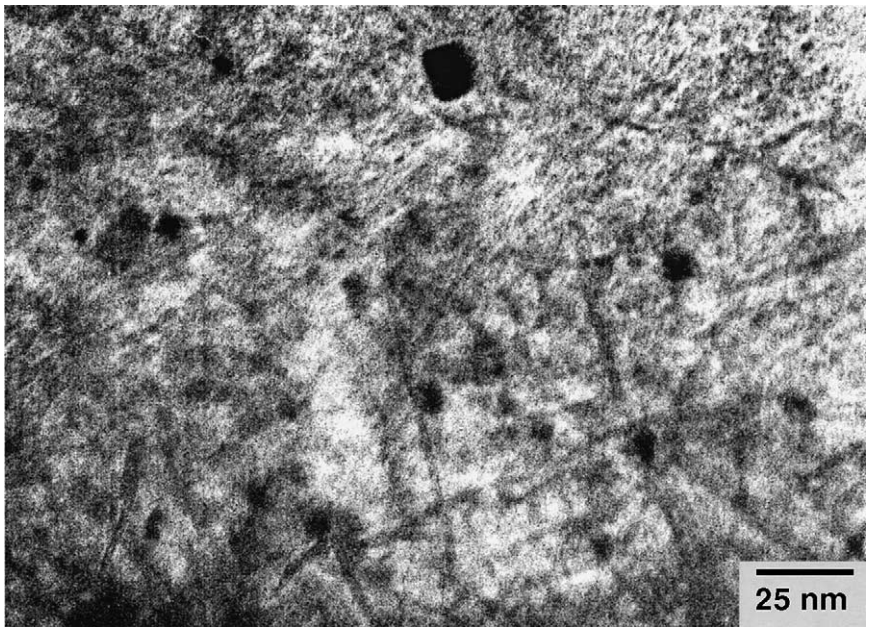

Fig. 4. Representative HRTEM micrograph of a catalyst spent under HC-SCR conditions (sample A1).

oxidized sites that can be reduced by propene is significantly larger for sample M2 than for sample M1. The shapes of propene response curves are hardly deviating from inert gas response curves (not shown). The reversible adsorptive interaction of propene with the catalyst is therefore negligible. The irreversible (reactive) adsorption of propene is apparently related to $Pt_{surf,redox}$ sites only.

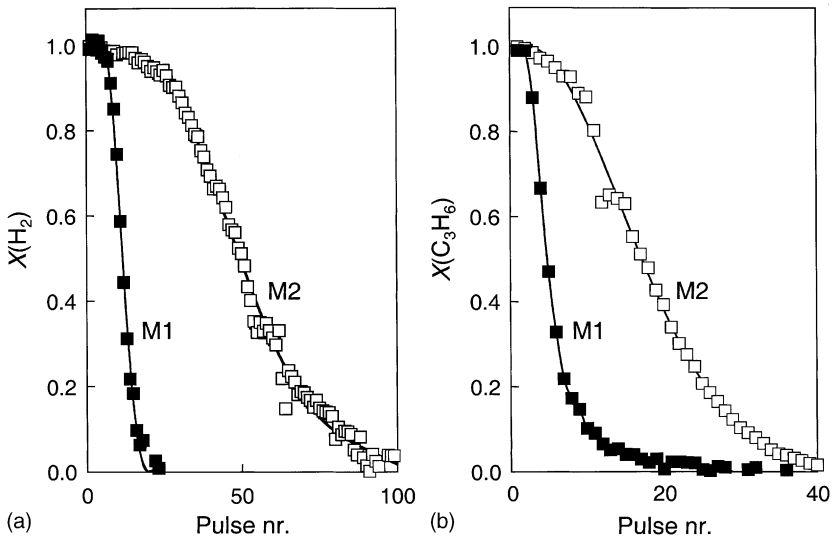

Fig. 5. Effect of Multitrack pretreatment procedures on the transient conversion of (a) hydrogen and (b) propene over the preoxidized catalyst M1 (solid symbols) and catalyst M2 (open symbols). Conditions: (a) pulsing pure H_2 over 100 mg catalyst at 523 K, $\sim 2 \times 10^{16}$ molecules per pulse, (b) 10 vol.% propene in Ar over 25 mg catalyst at 523 K, $\sim 5 \times 10^{16}$ molecules per pulse.

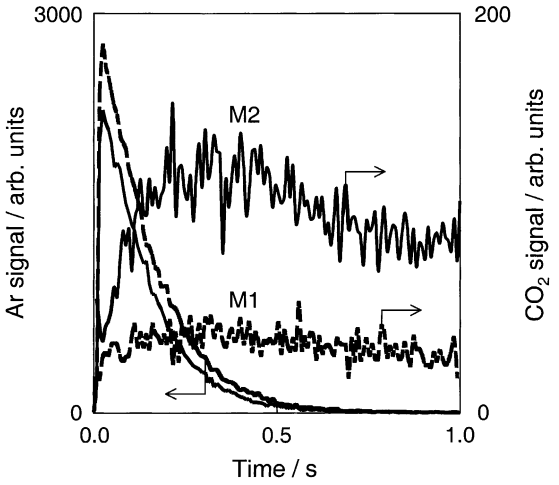

Fig. 6. Effect of Multitrack pretreatment procedures on the CO_2 single pulse response of 10 vol.% propene in Ar over preoxidised catalyst M1 (dashed lines) and catalyst M2 (solid lines). Conditions as described in Fig. 5b. Pulse with maximal CO_2 yield was selected.

Fig. 6 shows the CO_2 release curves as a result of the interaction of propene with the oxidized catalysts. As the CO_2 signal did not reach the baseline during the measurements, calculation of the carbon mass balance is not accurate. Nevertheless it can be estimated, that only a minor fraction (maximum 20%) of the adsorbed propene is transformed into CO_2, while a larger fraction of the adsorbed propene remains adsorbed on the catalyst as carbonaceous material (see Section 3.3.2).

The CO_2 curves are broadly compared to the response of inert gas. This is most likely due to a combined effect of the slow rate of CO_2 formation on the catalyst and a chromatographic effect of adsorption–desorption cylces of CO_2 on the alumina surface. It is quite likely that total combustion processes leading to CO_2 are relatively slow, since these require a long chain of intermediary reaction steps after the adsorption of propene on the oxidized Pt sites.

Fig. 6 also shows that transient CO_2 release over sample M2 is much higher than over sample M1, which is obviously a result of the higher amount of surface oxygen available for reaction with propene.

3.3.2. Re-oxidation

3.3.2.1. O_2 and NO uptake over H_2-reduced Pt surfaces. In Table 3, uptake values for O_2 and NO of catalysts M1 and M2 are summarized. In agreement with the reduction experiments shown in Fig. 5a, the treatment leading to catalyst M2 induced a dramatic increase of both O_2 and NO uptake on the hydrogen-reduced catalyst. For each O_2 molecule an equivalent of two and a half molecules NO are adsorbed on catalyst M1, and about two molecules NO on catalyst M2. This over-stoichiometric adsorption of NO on catalyst M1 will be further discussed in the following sections. The main product observed by exposing NO to the reduced Pt surfaces was N_2 (*m*/*e* 28). The yield of N_2 over catalyst M1 was in agreement with the oxygen uptake. Since neither water nor NH_3 were detected upon re-oxidation, the O_2 and NO uptake values are not affected by hydrogen that was irreversibly adsorbed on the catalyst.

3.3.2.2. NO uptake on oxidized Pt surfaces. NO was also pulsed over an O_2-preoxidized Pt surface of catalyst M1. In agreement with the experiments over Pt sponge performed by Lacombe et al. [27] the shape of a single pulse response of NO over an oxidized platinum catalyst is largely broadened compared to Ar (not shown). In an equivalent experiment over the pure support material, only a small difference in the width of the NO and Ar pulse was found. This shows that the peak broadening for NO is related to the platinum phase. Due to the interaction of NO with the oxidized Pt-surface, conversion into N_2 and N_2O was observed. Also the formation of NO_2 species that remain adsorbed on the catalyst is very likely [28]. The formation of N_2O and adsorbed NO_2 explain the over-stoichiometric NO uptake on sample M1 (see Table 3). On sample M2 the Pt surface hardly contains oxygen. Since the dissociation rate of NO is faster than reaction with surface oxygen, side reactions to N_2O or adsorbed NO_2 are limited. Consequently, the take up of NO is in closer stoichiometric agreement to the O_2 uptake values on catalyst M2.

3.3.2.3. O_2 uptake over C_3H_6-reduced Pt surfaces. Compared to a reduction with hydrogen reduction of the catalyst with propene leads to a three-fold increase of the total oxygen uptake (Table 3). The re-oxidation of the catalyst is accompanied by a large release of CO_2. Furthermore, compared to reduction with hydrogen, reduction of catalyst M1 with propene leads to a decrease in the oxygen conversion of the first

Table 3
O_2 and NO uptake during Multitrack titration experiments

Catalyst	O_2 uptake (10^{-9} mol mgCat^{-1})		NO uptake (10^{-9} mol mgCat^{-1})
	After H_2 treatment	After C_3H_6 treatment	After H_2 treatment
M1	1.9	6.5	4.8
M2	12	42	22
M2/M1	6.3	6.5	4.5

Table 4
Comparison of Multitrack titration data with CO chemisorption data

Catalyst	Pt dispersion	Pt_{surf}[a] (10^{15} atom mgCat^{-1})	$Pt_{surf,redox}$[b] (10^{15} atom mgCat^{-1})	$Pt_{surf,redox}/Pt_{surf}$
M1	0.73	23	2.3	0.1
M2	0.47	15	15	1.0

[a] Determined from the CO chemisorption experiments.
[b] Determined from the Multitrack titration data (H_2/O_2 cycle, Table 3).

pulse from 88 to 32%, and CO_2 was identified as a product (not shown). Apparently a large fraction of the redox-active Pt sites is covered by carbonaceous species, inhibiting the re-oxidation rate of reduced Pt particles. Assuming a linear relationship between the oxygen conversion in an O_2 pulse and the number of reduced Pt sites present in the Multitrack reactor [28], one can estimate that at least 75% of the active sites are covered with carbonaceous species. For catalyst M2 a decrease in O_2 conversion in the first pulse from 99 to 90% was observed. Since here the O_2 conversion in the first pulse after reduction with hydrogen is essentially 100%, it cannot be assessed what fraction of the catalyst is covered with carbonaceous deposit after reduction with propene.

Based on these results, it can be concluded that quantification of the number of redox-active Pt surface sites using propene as the reductant is not possible. To this end, hydrogen should be used. The relative increase of O_2 uptake upon treatment M2 is the same for hydrogen and for propene. Thus, the O_2 uptake upon H_2 treatment is taken as a measure for the number of sites participating in the redox cycle of total propene oxidation.

3.3.3. Platinum sintering: CO chemisorption versus Multitrack

CO chemisorption was applied to study the morphology of the samples M1 and M2 after the Multitrack experiments. The two experiments lead to a different degree of sintering: treatment M2 results in an increase of the apparent average Pt particle size from 1.3 to 2.7 nm, while by treatment M1 the platinum dispersion of the fresh catalyst is preserved.

Table 4 further indicates that all Pt_{surf} sites on catalyst M2, as determined by CO chemisorption, are participating in the H_2/O_2 cycles in the Multitrack experiments. On sample M1, however, only 10% of the Pt_{surf} sites are involved in the redox cycles.

4. Discussion

4.1. The effect of sintering on the redox activity of Pt particles

The results of the present study demonstrate that sintering of Pt particles occurs in the deNO_x reaction in plug flow reactors above 573 K, and in H_2 at temperatures of 773 K under Multitrack conditions. In agreement with the results reported in this study, various research groups observed sintering of Pt particles under HC-SCR conditions. Denton et al. [6] show that under reaction conditions severe sintering occurs over Pt/Al_2O_3 and Pt/SiO_2. Only supported on microporous silica Pt dispersions higher than 30% are preserved. Lööf et al. [7] show that treatment with 0.1 vol.% NO in Ar effectively induces sintering of small reduced

platinum particles (average $d_p < 2$ nm) at relatively low temperature ($\geq$473 K). Schneider et al. [8,9] confirmed this observation using X-ray absorption spectroscopy (XAS).

Under Multitrack (and TAP reactor) conditions, a significant fraction of the exposed Pt surface sites of small particles remains oxidized (PtO_{stable}), although these sites are reducible in the hydrogen pretreatment of the CO chemisorption experiments (performed with pure H_2, at 553 K, for 2 h). After sintering, this is not the case any more. There are two explanations possible for this result.

I. On sample M1, many Pt particles are located in small pores. In the Knudsen diffusion regime of the Multitrack, H_2 molecules do not reach their surface sites because of diffusion limitation. Besides particle growth, sintering leads to relocation of Pt particles in bigger pores with less diffusion limitation.
II. The chemical nature of PtO sites has changed due to sintering.

According to Huinink [29] and Nijhuis [30] diffusion limitations such as suggested by the first explanation are possible, if the characteristic time constant t_c of the mass transport through the bed (in Eq. (3): L_{bl} = bed length, $D_{part} = f$(particle radius) = coefficient of Knudsen diffusion through the catalyst bed) is orders of magnitude smaller than the characteristic time constant of the diffusion in the pores (in Eq. (4): L_{pd} = particle diameter, $D_{pore} = f$(pore radius) = coefficient of Knudsen diffusion through the porous particle).

$$t_c = \frac{L_{bl}^2}{D_{part}} \quad (3)$$

$$t_c = \frac{L_{pd}^2}{D_{pore}} \quad (4)$$

The comparison of these time constants can be reduced to relations of characteristic lengths in the reactor [30]. In our case (bed length: 1 cm, particle diameter: 200 μm, main pore radius 10 nm) both t_c values are estimably in the same order of magnitude, which induces an intermediate situation between complete absence of gradients and no penetration of the porous particle by the probe molecules at all. This intermediate situation may lead to a certain decrease of the effective reduction rate inside the center of the particle, but not to the extent that the hydrogen partial pressure in large sections of the catalyst particle is constantly zero. Furthermore, the relatively broad peak of the H_2 pulse response curve over the reduced samples indicates adsorption–desorption processes on reduced Pt surface sites. Any adsorptive interaction of the probe molecule by adsorption and desorption additionally increases the transient partial pressure gradient over the particle radius. This once more decreases the transport rate through the catalyst bed and increases the transport rate into the smaller pores.

Therefore, the first explanation can be dismissed. A change in the chemical nature of the PtO bond is the only feasible explanation.

During the H_2 treatment procedure in the Multitrack reactor (high vacuum, 473–573 K, ~2 min treatment duration) the partial pressure of hydrogen is extremely low, at least eight orders of magnitude lower than in the pretreatment of the CO chemisorption experiment. Under these low H_2 pressures, a difference between kinetic stabilities of PtO species becomes visible, while at the applied high H_2 pressures and long treatment periods in the pretreatment of the CO chemisorption this is not the case.

The ability to spare surface sites having a low reactivity is characteristic for our titration method under high vacuum and 'real life' reaction temperatures and its main difference to static volumetric H_2/O_2 titration.

Despite the lower operation temperature (near room temperature), the higher partial pressures of H_2 and the unlimited treatment period in static volumetric H_2/O_2 titration leads to the reduction of all Pt surface sites within the measuring period. However, this typical observation is not necessarily in conflict with our observation, that PtO_{stable} species are not reduced at 573 K under Multitrack conditions.

Suppose, the H_2 conversion at 573 K over PtO_{stable} sites would be 0.2% per pulse in Multitrack, which is too low to be determined. By approximating the mean residence time of H_2 with 0.1 s, a reaction rate constant can be estimated according to a differential reactor model ($k_{est} = \sim 6 \times 10^{-20}\ s^{-1}$). By considering the volumetric H_2/O_2 titration set-up as a semi-batch reactor with a constant hydrogen level of approximated 5 kPa and a reaction order of one for the partial pressure of hydrogen, only such a reaction rate constant is needed to estimate the half-life time of PtO_{stable}

species. Assuming a relatively low apparent activation energy like 12 kJ/mol, this half-life time could be still ~3 min at room temperature.

To assume such a low activation energy is not entirely unrealistic. Applying time-resolved EELS over oxygen covered Pt(1 1 1) reacting with gaseous H_2 at a temperature between 130 and 165 K, Germer and Ho [31] reported an activation energy of 11.7 kJ/mol for the formation of hydroxyl and 17.6 kJ/mol for the formation of water. If one considers the adsorption of H_2 as possible rate determining step, the apparent activation energy could even become lower. For modeling the hydrogen adsorption step during the H_2/O_2 surface reactions on polycrystalline Pt surfaces (900–1300 K) a sticking coefficient of $0.047\,s^{-1}$ and an activation energy of zero is considered [32,33]. Taken into account molecular beam experiments by Verheij and Hugenschmidt [34], even a negative apparent activation energy is possible, especially if activated adsorption (chemisorption) on the Pt metal is blocked by high oxygen coverage and, thus, non-activated adsorption is predominant.

As was already indicated in Section 1 of this paper, three hypotheses can be postulated to explain the increasing combustion activity as a function of increasing Pt particle size:

(I) Direct correlation of decreasing average PtO bond strength with TOF.
(II) The relative abundance of specific active surface sites on Pt metal particles.
(III) The relative abundance ionic oxygen associated with oxidized Pt particles versus atomic oxygen associated with metallic platinum.

Following the results of C_3H_6 treatment procedure in the Multitrack reactor, it is obvious that PtO_{stable} does not contribute to propene oxidation activity at all. In this sense, activation and particle size dependency cannot be explained without consideration of Pt sites or particles with different TOF. Thus, hypothesis (I) can be dismissed. Analyzing data given by Burch and Watling [35], one can find further support for the presence of inactive Pt surface sites on highly dispersed Pt/Al_2O_3. Their catalyst had a metal dispersion of 69% and was used to study transient NO decomposition at 513 K after reduction in a diluted hydrogen flow for at least 10 min. From the transient NO conversion data (related to N_2 yields) it can be estimated that not more than ~18% of the platinum surface sites after hydrogen reduction are available for fast NO dissociation. Note, that this calculation assumes the absence of Pt sintering.

The question remains, whether PtO_{stable} can be assigned to oxygen adsorbed on edge and corner positions (relates to second hypothesis) or to ionic oxygen species (relates third hypothesis).

Hypothesis (II) was, among others, discussed by Carballo and Wolf [12], who suggested a lower activity of metal sites on edge and corner positions in propene oxidation than on associated terrace sites as an effect of higher binding energy of oxygen. Accordingly propene is oxidized preferably over terrace sites, whose relative concentration is lower on small particles than on big particles. This picture was disputed on bases of surface science studies of oxygen over stepped Pt surfaces [15,36]. However, recent studies over Pt(3 3 5) surfaces clearly demonstrate that oxygen species on step sites have higher desorption temperatures than on terrace sites, and thus a higher stability [20]. To further validate this theory as an explanation of the experimental results of the present work, a cuboctahedral shape of semi-hemispherical model particles is postulated to represent the catalyst particles in the applied catalysts (see Fig. 7a). The solid line in Fig. 7b illustrates the calculated relative amount of Pt terrace sites as a function of increasing Pt particle size. If only the terrace sites ($Pt_{surf,terrace}$) would be active in redox cycles in Multitrack conditions ($Pt_{surf,redox}$), the points M1 and M2 indicated in Fig. 7b should coincide with the calculated line. Clearly, the high (100%) reducibility of sample M2 does not confirm to the model. In fact, the Multitrack data of sample M2 suggest that an average d_p of 2.7 nm is sufficient to enable redox activity of all available Pt_{surf} sites, while according to the cuboctahedral model still a large fraction of edge-sites exists.

The Multitrack results imply that a certain transition of all the sites from redox inactivity to redox activity exists. This is most likely the result of a transition in the type of oxygen that is adsorbed on the Pt particles. It thus appears that hypothesis (III) is most likely. On particles smaller than approximately 2.7 nm the oxygen can be ionic in character and, thus, inactive. Above this size only atomic oxygen is present, which can readily oxidize hydrogen and propene. In other words, the small and oxidized Pt particles have

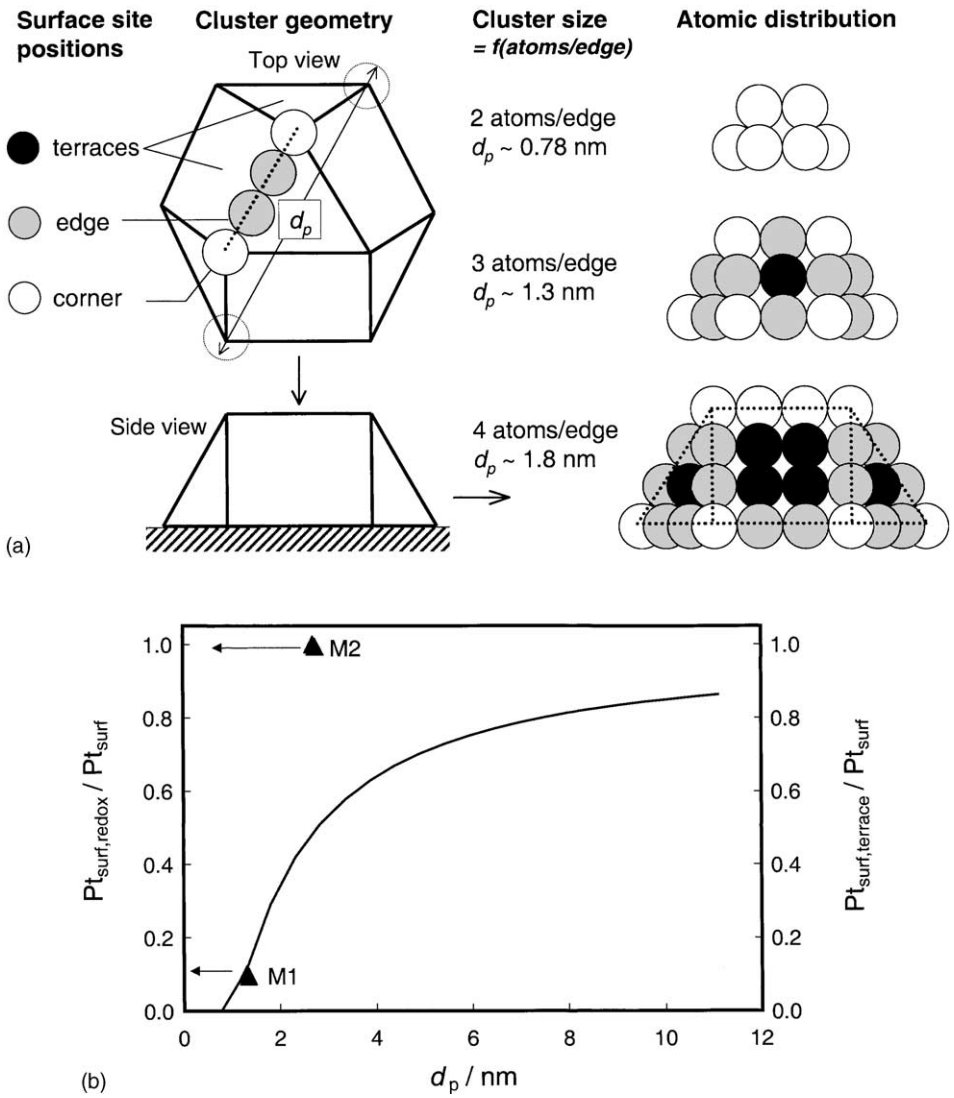

Fig. 7. (a) Semi-cuboctahedral model for Pt particles: geometry and types of surface sites, (b) the fraction of terrace surface sites ($Pt_{surf,terrace}/Pt_{surf}$) in dependence of the size of a semi-cuboctoctahedral model particle (no symbol). Comparison of $Pt_{surf,terrace}/Pt_{surf}$ with the ratio of reactive and unreactive Pt surface sites ($Pt_{surf,redox}/Pt_{total}$) according to Multitrack titration data (solid symbols).

a limited metallic character. Note, that this metallic character is a necessity for chemisorption of H_2, so only non-activated adsorption of H_2 is possible over PtO_{stable}. In the view of the previous comparison of H_2/O_2 titration procedures at different temperatures, it is justified to assume a reaction order of one and a small (even negative) activation energy.

It is clear, that the small fraction of large Pt particles shown in Fig. 2b is metallic. Their Pt surface sites are supposed to be redox active. It is, however, not clear, if small sized particles shown in Fig. 2a belong to the fraction of metallic redox-active Pt particles on catalyst fresh and M1.

Briot et al. [14] investigated a higly dispersed Pt/Al_2O_3 catalyst, which they claimed to be free of any large Pt particles based on their TEM micrographs. The reducibility of Pt/Al_2O_3 catalysts was assessed using H_2-TPR. After sintering, they found a shift

in the H_2 reduction temperature from above 270 K (high dispersion) to 195 K (low dispersion), which they could correlate with a loss of average oxygen binding energy of about 30 kJ/mol. In resemblance to our results, they further reported a small fraction of the highly dispersed Pt/Al_2O_3 to be reduced already at 195 K (~10%), suggesting the presence of some more redox-active Pt particles.

4.2. Redox activity of Pt particles and the oxidation of C_3H_6

The Multitrack data clearly demonstrate that PtO_{stable} sites do not participate in the strong adsorption of C_3H_6 and the oxidation of the adsorbed carbonaceous species at temperatures around 523 K. Only $Pt_{surf,redox}$ sites could be active sites for propene oxidation at that temperature, as both parts of the catalytic cycles are fast.

As discussed in the previous section, the PtO_{stable} sites probably have an ionic character. As such their ability to oxidize might be decreased. More importantly perhaps, the corresponding Pt particles have a limited metallic character. The activated chemisorption of both H_2 and C_3H_6 on Pt metal is based on the interaction between d-electrons of the Pt phase and the molecules' anti-bonding σ^* orbitals or π_z^* orbitals, respectively.

These two effects caused by the small particle size would explain why H_2 and C_3H_6 are equally unable to remove oxygen from PtO_{stable} sites, creating reduced Pt_{surf} sites. Without that step, no significant catalytic cycle can be established.

4.3. Activity of Pt catalysts in the HC-SCR reaction

In agreement with many other studies the particle size was found to affect the NO_x conversion in steady state conditions. Fig. 8a shows the NO_x conversion at 523 K as a function of Pt dispersion. A maximum conversion is reached at an intermediate dispersion. At low dispersions the activity is limited by a decreasing number of Pt_{surf} sites. If the Pt dispersion becomes too high, in view of the Multitrack results, the low activity of the catalyst is related to the low reducibility of oxidized Pt sites.

In the previous section, it was discussed that PtO_{stable} sites cannot be transformed into reduced Pt

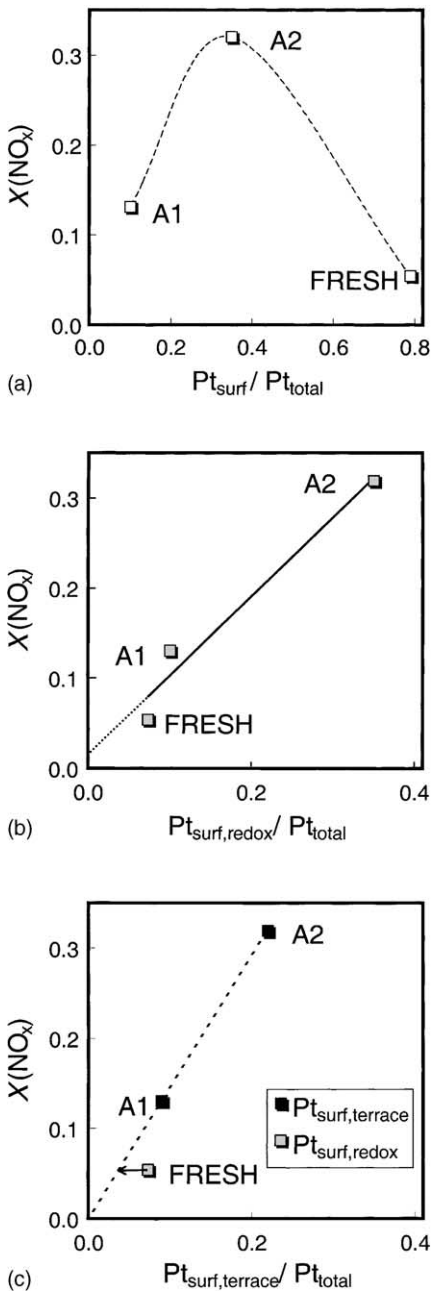

Fig. 8. NO_x conversion at 523 K related to Pt surface sites (a) according to CO chemisorption (Pt_{surf}/Pt_{total}, open symbol), (b) applying Multitrack results for distinction of active and inactive surface sites ($Pt_{surf,redox}/Pt_{total}$, grey symbols, solid trendline), and (c) the theoretically calculated fraction of Pt surface terrace sites ($Pt_{surf,terrace}/Pt_{total}$, solid symbols, dotted trendline). Linear trendlines were calculated without setting an interception. For reaction conditions, see Fig. 3.

sites by C_3H_6 at reaction temperatures. NO reduction during HC-SCR over Pt catalysts can be related to two general pathways, which have been proposed for the complete catalytic cycle. For both proposals, reduced Pt sites are essential:

1. Reduced Pt sites are competitively oxidized by NO or O_2 [2,5,37], while propene removes adsorbed oxygen to regenerate the reduced surface (clean-off mechanism).
2. Reduced Pt sites are necessary for strong adsorption of NO and propene to enable the formation of N-containing organic compounds, which serve as N–N-coupling intermediates [38].

It was demonstrated by the experiments with propene in Multitrack conditions that strong interactions with the Pt surface occur, yielding carbonaceous deposits on the catalyst. In view of the lower oxygen conversion per pulse after reduction in propene, compared to reduction in H_2, it can be assessed that at least part of the carbonaceous deposit is located on $Pt_{surf,redox}$ sites. Given the ability of $Pt_{surf,redox}$ sites to adsorb NO without immediate dissociation, not only NO dissociation is a realistic pathway for HC-SCR over $Pt_{surf,redox}$ sites, but also reaction of NO with carbonaceous deposits to form N-containing organic compounds. The NO and propene titration experiments on catalyst M1 further indicate that neither the support nor the PtO_{stable} site contribute largely to irreversible adsorption and activation of NO.

In any case, the conclusion can be drawn, that HC-SCR is possible exclusively over $Pt_{surf,redox}$ sites. The following points further support this conclusion:

- The activation of the catalyst does not influence the hydrocarbon efficiency as reaction (1) and (2) are activated simultaneously.
- If only the redox-active fraction (as determined by Multitrack, i.e. $Pt_{surf,redox}/Pt_{surf}$ of $\sim$0.1) of the highly dispersed catalyst (fresh) is considered, a linear relation between the dispersion and TOF can be obtained (Fig. 8b).

Considering the latter point, there is significant scattering in the data points in Fig. 8b. This indicates that $Pt_{surf,redox}$ sites are not equivalent in their contribution to HC-SCR activity which is suggesting structure sensitivity (please note here the assumption that for samples A1 and A2 $Pt_{surf,redox}$ equals Pt_{surf}). In Fig. 8c, the dispersion of catalysts A1 and A2 is corrected for the theoretical fraction of terrace sites, according to the model presented in Fig. 7. For the low dispersed sample A1 this results in a small correction ($Pt_{surf,terrace} \sim 0.9\ Pt_{surf}$), while for the higher dispersed sample A2 the correction is large ($Pt_{surf,terrace} \sim 0.6\ Pt_{surf}$). When the NO conversion is plotted against the parameter $Pt_{surf,terrace}/Pt_{total}$ the extended correlation line intercepts the *y*-axis at zero conversion (Fig. 8c), which is not the case for the extended correlation line in Fig. 8b. This suggests that once an average particle size is reached where all the sites are redox-active (in Multitrack conditions), $Pt_{surf,terrace}$ sites could be preferred as active sites in the HC-SCR reaction at steady state conditions.

For the fresh catalyst, the corrected dispersion of 0.073 is based on an average of the (small) fraction of active particles ($Pt_{surf,redox}/Pt_{surf}$) and the large fraction of inactive particles ($d_p <\sim 2$ nm). In Fig. 8c the correction, which one would need to transpose the activity of the active Pt_{surf} fraction of the fresh catalyst to the line corresponding to the activity of the $Pt_{surf,terrace}$, is indicated by the arrow ($Pt_{surf,terrace} \sim 0.5\ Pt_{surf,redox}$). Using this $Pt_{surf,terrace}/Pt_{surf,redox}$ ratio of 0.5 on the theoretical line in Fig. 7, the average particle size of the active fraction of the fresh catalyst can be estimated to be 2.8 nm. This indicates that besides the very large particles observed in Fig. 2b, also smaller particles (but larger than 2 nm!) in the fresh catalyst are contributing to the NO_x conversion. Please note, that this conclusion is only valid, if the suggestion of $Pt_{surf,terrace}$ sites on redox-active platinum particle being the active site is correct.

Summarizing, the performance of Pt/Al_2O_3 catalysts in HC-SCR is the result of (i) a minimum required Pt particle size of about 2.7 nm for activity, below which the particles may become oxidized and inactive and (ii) the terrace fraction of the particles larger than 2.7 nm. Please note that this trend is valid for Pt/Al_2O_3 catalysts, while for other platinum catalysts the correlation of the activity with the amount of terrace sites is not the only factor determining the obtained lean $deNO_x$ activity [39].

Further validation of the mechanism and the role of the Pt dispersion on activity is necessary, by performing kinetically-controlled catalytic tests, yielding the dependency of the reaction order and the apparent activation energy on the metallic dispersion, as was

shown by Garetto and Apesteguia [16] for benzene oxidation. These experiments will be performed in the near future.

5. Conclusions

The following conclusions can be derived from this study:

- H_2/O_2 titration cycles in the Multitrack can be used to quantify $Pt_{surf,redox}$ sites on Pt/Al_2O_3. Due to the extremely low partial pressure of hydrogen, tightly bound oxygen (PtO_{stable} sites) associated with small Pt particles is not reactive at temperatures of 573 K in Multitrack conditions.
- An apparent transition in reduction behavior exists at an average Pt particle size of about 2.7 nm, where all types of surface sites (terraces, edges, kinks and corners) become redox active. This transition might be related to the nature of the oxygen that is associated with the Pt particles, changing from ionic to atomic type oxygen species.
- All reduced $Pt_{surf,redox}$ sites can be oxidized by NO producing mainly N_2.
- If propene is used as the reducing agent, carbonaceous deposits are formed over redox-active Pt sites, which can be removed easily by subsequent reaction with O_2.
- Activation of propene oxidation and HC-SCR by sintering of small Pt particle is due to (i) a minimum required Pt particle size of about 2 nm for activity, below which the particles are completely inactive and (ii) an increase in the relative terrace fraction of the particles larger than 2 nm. This is valid, irrespective of the mechanism explaining the HC-SCR pathway.

Acknowledgements

This research was financially supported by the Council for Chemical Sciences of The Netherlands Organization for Scientific Research (CW-NWO). B.V.D. Linden and P.J. Kooyman are gratefully acknowledged for assistance in the Multitrack experiments and performing the TEM experiments, respectively. G. Mul gratefully acknowledges a fellowship granted by the Royal Netherlands Academy of Arts and Sciences.

References

[1] Y. Traa, B. Burger, J. Weitkamp, Micropor. Mesopor. Mater. 30 (1999) 3.
[2] J. Pérez-Ramírez, J.M. García-Cortés, F. Kapteijn, G. Mul, J.A. Moulijn, C. Salinas-Martínez de Lecea, Appl. Catal. B 29 (2001) 285.
[3] G. Centi, S. Perathoner, F. Vanazza, CHEMTECH 12 (1999) 48.
[4] R.J. Farrauto, R.M. Heck, Catal. Today 51 (1999) 351.
[5] R. Burch, P.J. Millington, Catal. Today 26 (1995) 185.
[6] P. Denton, A. Giroir-Fendler, H. Praliaud, M. Primet, J. Catal. 189 (2000) 410.
[7] P. Lööf, B. Stenbom, H. Norden, B. Kasemo, J. Catal. 144 (1993) 60.
[8] S. Schneider, D. Bazin, F. Garin, G. Maire, M. Capelle, G. Meunier, R. Noirot, Appl. Catal. A 189 (1999) 139.
[9] S. Schneider, D. Bazin, G. Meunier, R. Noirot, M. Capelle, F. Garin, G. Maire, Catal. Lett. 71 (2001) 155.
[10] K. Otto, H.C. Yao, J. Catal. 66 (1978) 229.
[11] E. Xue, K. Seshan, J.R.H. Ross, Appl. Catal. B 11 (1996) 65.
[12] L.M. Carballo, E.E. Wolf, J. Catal. 53 (1978) 366.
[13] M.C. Demicheli, L.C. Hoang, J.C. Menezo, J. Barbier, M. Pinabiau, Appl. Catal. A 97 (1993) L11.
[14] P. Briot, A. Auroux, D. Jones, M. Primet, Appl. Catal. 59 (1990) 141.
[15] R.F. Hicks, H. Qi, M.L. Young, R.G. Lee, J. Catal. 122 (1990) 280.
[16] T.F. Garetto, C.R. Apesteguia, Appl. Catal. B 32 (2001) 83.
[17] T.F. Garetto, C.R. Apesteguia, Catal. Today 62 (2000) 189 (and references therein).
[18] B.E. Nieuwenhuys, Adv. Catal. 44 (2000) 259.
[19] R. Burch, M.J. Hayes, J. Mol. Catal. A 100 (1995) 13.
[20] H. Wang, R.G. Tobin, D.K. Lambert, C.L. DiMaggio, G.B. Fisher, Surf. Sci. 372 (1997) 267.
[21] A. Borgna, F. Le Normand, T. Garetto, C.R. Apesteguia, B. Moraweck, Catal. Lett. 13 (1992) 175.
[22] H. Lieske, G. Lietz, H. Spindler, J. Volter, J. Catal. 81 (1983) 8.
[23] R.W. McCabe, C. Wong, H.S. Woo, J. Catal. 144 (1988) 354.
[24] T.A. Nijhuis, L.J.P. van den Broeke, M.J.G. Linders, M. Makkee, F. Kapteijn, J.A. Moulijn, Catal. Today 53 (1999) 189.
[25] E.P. Barrett, L.G. Joyner, P.H. Halenda, J. Auer, JACS 79 (1951) 379.
[26] J. Pérez-Ramírez, R.J. Berger, G. Mul, F. Kapteijn, J.A. Moulijn, Catal. Today 60 (2000) 93.
[27] S. Lacombe, J.H.B.J. Hoebink, G.B. Marin, Appl. Catal. B 12 (1997) 207.
[28] A.R. Vaccaro, G. Mul, J.A. Moulijn, Stud. Surf. Sci. Catal. 133 (2001) 357.
[29] J.P. Huinink, Ph.D. Thesis, Eindhoven University of Technology, Eindhoven, 1995.

[30] T.A. Nijhuis, Ph.D. Thesis, Delft University of Technology, Delft, 1997.
[31] T.A. Germer, W. Ho, Chem. Phys. Lett. 163 (1989) 449.
[32] S. Ljungström, B. Kasemo, A. Rosén, T. Wahnström, E. Fridell, Surf. Sci. 216 (1989) 63.
[33] M. Försth, Combust. Flame 130 (2002) 241.
[34] L.K. Verheij, M.B. Hugenschmidt, Surf. Sci. 416 (1998) 37.
[35] R. Burch, T.C. Watling, Catal. Lett. 37 (1996) 51.
[36] J.L. Gland, Surf. Sci. 93 (1980) 487.
[37] J. Pérez-Ramírez, J.M. García-Cortés, F. Kapteijn, G. Mul, J.A. Moulijn, C. Salinas-Martínez de Lecea, Appl. Catal. B 29 (2001) 285.
[38] G.R. Bamwenda, A. Ogata, A. Obuchi, J. Oi, K. Mizuno, J. Skrzypek, Appl. Catal. B 6 (1995) 311.
[39] J.M. García-Cortés, J. Pérez-Ramírez, A.R. Vaccaro, J.N. Rozaud, M.J. Illán-Gómez, C. Salinas-Martínez de Lecea, J. Catal. 218 (2003) 111.